RF SUPERCONDUCTIVITY AT ORSAY

V. Nguyen Tuong, L. Wartski, M. Boussoukaya,
K.M'Baye, M. Pham Tu and J.C. Villegier*

Institut d'Electronique Fondamentale
Laboratoire associé au CNRS Bât. 220
Université Paris-Sud, 91405 Orsay-Cédex, F.

At Orsay, after carrying out experiments on field emission from oxidized Nb at low temperature, secondary emission of Ti and C coated Nb and multipactoring in rf coaxial reentrant cavities, activities have been recently devoted to the problem of surface cleaning using UV/ozone technique in Nb S-band cavities and to the studies of NbN films.

I. INVESTIGATIONS OF S-BAND NIOBIUM CAVITIES

Measurements at 2.9 GHz on TM mode superconducting Niobium cavities have been carried out in an attempt to show the effectiveness of the ultra-violet/ozone cleaning method on the RF performances. It is generally recognized that clean surface plays a primordial role in attaining high Q and high fields in superconducting cavities. Heating above 2000°C in UHV was shown to be quite effective in cleaning Niobium surface[1] but this method is expensive and practically inadequate for large cavities or structures. On the other hand, the UV/Ozone cleaning process has been successfully used on a variety of surfaces including : glass, sapphire, semiconductors and metals, especially when contaminants are hydrocarbons. R. Sowell[2] et al. reported that prolonged exposure to UV radiation produced clean surfaces on gold and glass in ambient air, as well as in a vacuum system. As shown in figure 1, the effectiveness of exposing gold contacts to UV radiation at a pressure of 10^{-4} Torr of oxygen is equivalent to the normal ultra-high vacuum bakeout procedures (200°C, 10^{-10} Torr) followed by sputter cleaning in argon. Also shown, to a different scale, is the recontamination of UV-cleaned gold contacts in normal laboratory air.

* I.E.T.I., CEA 85 X - 38 041 Grenoble, F.

(presented by V. Nguyen- Tuong)

UV/Ozone cleaning is the result of photosensitized oxidation processes[2] as indicated schematically in figure 2. The contaminant molecules are excited and/or dissociated by the absorption of short wavelength UV-light. Simultaneously, atomic oxygen and ozone are produced when O_2 is dissociated by the absorption of UV with a wavelength less than 2454 A. Atomic oxygen is also produced when ozone is dissociated by the absorption of the UV and longer wavelength of radiation. The excited contaminant molecules, and the free radicals produced by the dissociation of contaminant molecules react with atomic oxygen to form simpler volatile molecules, such as CO_2, H_2O, N_2, etc.

A convenient radiation for producing O_3 is the 1849 Å wavelength emitted by low pressure Hg discharge lamps in fused quartz envelopes. Similarly, since most hydrocarbons have a strong absorption band between 2000 Å and 3000 Å, the 2537 Å wavelength emitted by the same lamps are useful for exciting or dissociating contaminant molecules.

To show the effects of this process, two samples of Niobium were chemically polished, rinsed with demineralized water and methanol. One was placed during one week inside an aluminium box approximately 1 cm from à 2 W low pressure mercury discharge lamp which generate the two wavelengths of interest, 1849 Å and 2537 Å, in order to receive prolonged UV/Ozone cleaning. Auger electron spectroscopy as well as glow discharge optical emission spectrometry show that UV/Ozone cleaning reduced considerably the carbon peak while increasing the Oxygen one.

Experiences on TM_{010} mode S-band Niobium single cavities were carried out on Stanford type[4] as well as on spherical CERN type cavities[5]. Chemical polishing was done in a standard $\frac{1}{3}$ HF + $\frac{1}{3}$ H NO_3 + $\frac{1}{3}$ H_3PO_4 solution followed by H_2O and methanol rinsing. UV/Ozone cleaning was applied to the cavities during 3 days by inserting a cylindrical 2 watt UV-lamp through the beam holes. The time exposure could be greatly reduced by using a more powerful UV tube.

The results are summarized in table 1 and 2. Exposures to dust free air at room temperature always lead to a degradation of RF performances which are recovered by chemical polishing. The same results are simply obtained by UV/Ozone cleaning instead of chemical polishing. When the UV/Ozone cleaning is applied just after chemical polishing, the RF performances are improved and these performances are almost conserved even after exposure to air. This could

be explained by the presence of a clean protective layer of Nb_2O_5 due to the UV/Ozone cleaning process itself.

In conclusion, UV/Ozone cleaning procedure appears to be an effective method to produce clean surfaces at room temperature and in room atmosphere. Moreover, clean surfaces will remain clean during exposure to UV/Ozone. It is a simple and inexpensive process, easy to set up and operate. It seems to be a promising in-situ self cleaning technique for RF cavities in a storage ring where UV photons are present due to synchrotron radiation.

II. PREPARATION AND CHARACTERISATION OF HIGH-RATE DC-MAGNETRON SPUTTERED NbN FILMS

As is well known, the RF surface resistance at a given temperature is exponentially lower with higher critical temperature T_c. In recent years, many investigators working on high T_c superconducting materials have outlined the attractive features, as far as high and reproducible T_c and H_{c2} are concerned, of Niobium Nitride (NbN), a B_1 structure compound, having the rock salt crystal structure. On the other hand, comparative studies, by Padamsee, between superconducting materials such as Nb, Nb_2O_5 coated Nb, A15 compounds such as Nb_3Sn and NbN, have shown that the latter has the lowest secondary electron emission coefficient[6]. Moreover NbN exhibits rather good immunity against external agents and radiation damage.

All these reasons have encouradged us, at Orsay, to develop a program with the LETI at Grenoble and devoted to RF surface cavity preparation and characterization of these NbN films at 9-10 GHz.

Surface preparation

In our preliminary experiments, the NbN films have been deposited on a Nb end-plate of a X-band TE_{011} mode bulk Nb cavity. Films deposition was carried out by means of a reactive DC magnetron sputtering method using a Nb cathode and an argon-nitrogen mixture. Substrate temperature was in the range of 300-500°C and typical deposition rates were 4 nm/s for a 5 kw target power. These deposition rates are about one order of magnitude faster than ordinary sputtering methods which lead to contamination of the film because of the long deposition times and to the difficulty in producing thick enough films for practical applications.

The residual pressure was maintained at less than 8 10^{-8} torr during full cryopumping and less than 4 10^{-7} torr with the throttle valve partially opened.

Carreful optimization of sputtering conditions was carried out in order to obtain high T_c values (15-16 K). Fig. 3 shows, as an example, the critical temperature T_c and low temperature (i.e. just above T_c) resistivity versus the nitrogen pressure which could be varied between 0 and 7 mTorr, and for two different fixed Ar pressure.(7)

It is seen that high T_c δ-NbN appears clearly for $P_{N2} > 4.10^{-3}$ torr and show maxima at T_c = 15.2 K for P_{N2} = 4.5 10^{-3} torr and P_{AR} = 5 10^{-3} torr. Even a higher T_c is obtained : T_c = 16.1 K, for P_{N2} = 5.5 10^{-3} torr and P_{AR} = 15.10^{-3} torr.

At lower nitrogen concentrations, the β-Nb_2N phase appears, mixed to the α-Nb phase.

Table III summarizes the sputtering optimized conditions for a set of seven NbN films.

TABLE III.

Power (kw)	4.5 to 5.7
Target voltage (V)	300 to 365
Substrate temperature (°C)	350
P_{N2} (mtorr)	5.5
$P_{AR} + N_2$ (mtorr)	19
Thickness (nm)	360 to 1500

Measurement methods and preliminary results.

The critical temperature of each sample was measured by two different methods : a four-probe resistive technique and an inductive method derived from Schawlov-Devlin's one.(8) In the latter, the disc-shaped sample is located between two coaxial-coils connected in series and constituting the inductive part of a resonant circuit. A tunnel diode is suitably biased by a constant voltage, so as to deliver a signal at a frequency ranging from about 50 kHz to 1 MHz. Sample and coils are put in a sealed box and immersed in a cryostat, and the temperature can be slowly varied in a wide range from 4.2 K up to 20 K. Carbon resistors are inserted inside the sample or fixed on it and provide temperature measurements with a precision better than 0.01 K. The residual resistivity just above T_c (at ≃20 K) was calculated from square resistance and thickness measurements.

As mentioned above, RF measurements are performed using a TE_{01n} mode (n = 1 or 2) resonator which is assembled from two parts : the Nb main body comprising the cylindrical part with one bottom-plate, and removable NbN coated end-plate.

The cavity is attached to the bottom of a vacuum can immerged in the helium bath while four identical lids covered with different layers are inserted into a barrel situated above the cavity. Heaters are placed inside each lid bearer so as to allow separate warming up of the lid. To minimize thermal contact and heat transfer towards the cylindrical body of the cavity, the lids were provided with knife-edge on the cavity side. Temperature measurements were performed by carbon resistors inserted in each lid and on the body of the cavity.

The penetration depth and Q factor were measured using an out-of-thermal equilibrium method : the temperature T_o of the body of the resonator was maintained constant while the temperature of the lid was rapidly raised from T_o to T. The subsequent frequence shift ΔF and reflected power is then registered so that:

$$\lambda_o = \frac{\Delta F}{\Delta y} \cdot 4 F_o \frac{L^3}{C^2}$$

with : $\lambda = \lambda_o \left\{1 - (T/T_c)^4\right\}^{-1/2} = \lambda_o y$

Fo is the resonant frequency of the cavity, L its length and $\lambda_o = \lambda(T=0)$. Fig. 4 shows the $\Delta\lambda(y)$ plot from which the values of λ_o is obtained. The precision of the method has been estimated to $\pm$ 100 Å.

This result is in excellent agreement with the one recently reported by S. Kubo et [9] who obtained $\lambda_o = 3060 \pm 100$ Å using a transmission line technique at 4.2 K to characterize by other means reactive Dc-magnetron sputtered films, and is very short compared with previously reported values [10]: (5000 Å < λ_o < 7000 Å). In ref [9], it has been pointed out that this very short λ value, indicating improvement in quality of the film, results from low-energy deposition inherent in magnetron sputtering and from impurity-free condition owing to comparably high rate deposition as well as the evacuation equipment used.

The $\Delta\lambda$ (y) plot in fig. 4 exhibits a strong deviation from the BCS theory for low temperatures. This can be accounted for by weak superconducting regions or "bad-spots" having roughly a critical temperature $T_c^* \simeq 7.5$ K. At higher temperatures, the contribution of these regions to the total penetration depth is temperature-independant and is represented by $\Delta\lambda_1 \simeq 230$ Å. This discrepancy between experiments and theory has been widely studied for Nb and is related to surface inhomogeneities coming from hydrogen or oxygen inclusions. Hydrogen is

absorbed from etchant during electro-or chemical- polishing processes [10] and oxygen results from oxydization or migration from the inner part of the sample during cooling from high temperatures in UHV untill room temperatures [11-13]. The explanation of this effect for the NbN case is less straight forward, due to the complexity of the NbN phase diagram and because the superconducting properties of NbN are strongly dependent on its composition and structure [14-15]. Phase transitions can occur between high-T_c δ phase and lower -T_c phases, and many different phases may coexist. All these phenomena contribute to lower the transition temperature and to increase the penetration depth.

Concerning the measurement of the surface resistance R_S of the NbN films, it was observed that the Q factor of the TE_{011} resonator in the presence of the NbN coated end-plate, at a temperature $T < T_c/2$, was essentially the same than the Q factor in the presence of the bulk Nb end-plate at 4.2 K. This is due to the small contribution of the end-plate to the overall losses.

At higher temperatures, measurements were possible and the R_S of NbN was deduced from the relation :

$$\frac{1}{Q} = \frac{R_S}{G} + \frac{R_{So}}{G_o} \qquad (G = 10\ 825\ \Omega \quad ; \quad G_o = 839\ \Omega)$$

R_{So} being the surface resistance of the Nb body of the cavity maintained at $T_o \simeq 5$ K.

Fig. 5 represents the variation of R_S as a function of the inverse of the reduced temperature.

The electrical properties of the NbN films are summarized in Table IV :

TABLE IV.

Superconducting Transition temperature :	15.9 K
Residual resistivity at 20 K :	585 μΩ cm
RRR ($\rho^{300\ K}/\rho_{20\ K}$) :	0.8
RF Surface resistance at 10 K:	$6.5\ 10^{-4}\ \Omega$
Measured penetration depth $\lambda_{o(0)}$:	375 nm
Calculated penetration depth $\lambda_c(0)$:	360 nm

Other experiments allowing measurements in an extended temperature range are planed with a short X-band TE_{011} cavity on which deposition of NbN films on the inner surface by the same technique is expected to be homogeneous enough. It is also planed to measure NbN films deposited on mirrors end-plates in a Fabry-Perot configuration at higher frequencies.

Acknowledgements

The authors are greatly indebted to P. Bernard, H. Lengeler and all the members of the CERN group for their aid and interest throughout the entire work.

TABLE I - EXPERIMENTAL RESULTS OF STANFORD TYPE S-BAND CAVITIES

Treatment	Q_o (1.6 K)	E_p (MV/m)	Conclusions
Chemical polishing (CP)	1.7×10^9	15.4	Q degradation
Exposed to dust free air at room temperature	4.7×10^7		
Chemical polishing	1×10^9	17	Performances almost recovered
Exposed to air then CP again	0.9×10^9	13.5	
Chemical polishing	1.3×10^9	14	Performances recovered
Exposed to air then UV/Ozone	1.3×10^9	13.7	
CP + UV/Ozone	4.9×10^9	19	Performance improved
Exposed to air	3.2×10^9	17.5	Performance almost conserved

TABLE II - EXPERIMENTAL RESULTS OF CERN TYPE S-BAND CAVITIES

Treatment	Q_o (1.6 K)	E_p (MV/m)	Conclusions
Chemical polishing (CP)	2.5×10^9	17.3	Degradation
Exposed to dust free air at room temperature	1.5×10^8	8.9	
Chemical polishing	1.6×10^9	14.2	Performances almost recovered
Exposed to air then CP again	1.4×10^9	12.5	
Chemical polishing	2.6×10^9	17.6	Performances recovered
Exposed to air then UV/Ozone	2.5×10^9	17.6	
CP + UV/Ozone	7.3×10^9	21.3	Performance improved
Exposed to air	6.2×10^9	20.8	Performance almost conserved

REFERENCES.

1. A. Septier, Proc. Workshop on RF superconductivity Karlsruhe, 1980 p.53-84.
2. R.R. Sowell, R.E. Cuthrell, D.M. Mattox, and R.D. Bland
J. Vac. Sci. Technol., Vol. 11, n° 1, Jan/Feb. 1974 p. 474-475.
3. J.R. Vig., Surface contamination. Edited by K.L. Mittal
Plenum Press NY 1979, p. 235-253.
4. C. Lyneis, Y. Kojima, J-P. Turneaure and Nguyen Tuong Viet
IEEE, Trans. on Nuclear Science NS 20, June 1973, p. 101-103.
5. U. Klein, D. Proch and H. Lengeler
Gesamthochschule Wuppertal, Internal Report WU B 80-16, May 1980.
6. H. Padamsee, A. Joshi, J. Appl. Phys. 50, 1112 (1979).
7. J-C. Villegier, J-C. Veler
IEEE Trans on Mag., Vol. Mag-19, n° 3, May 1983.
8. A.L. Schawlow, G.E. Devlin
Phys. Rev. 113, 120 (1959).
9. S. Kubo, M. Asahi, M. Hikita, M. Igorashi
Appl. Phys. Lett. 44 (2), 15 january 1984.
10. S. Isagawa , J. Appl. Phys. 52 (2) February 1981.
11. W. Schwarz, J. Halbritter, J. Appl. Phys. 48, 4618 (1977).
12. J. Halbritter, J. Appl. Phys. 46, 1403 (1975).
13. N. Schroeder, Dissertation, Freiburg (1980).
14. R.W. Guard, J.W. Savage, D.G. Swarthout,
Trans Metall. Soc. AIME 239, 643 (1967).
15. L.E.Toth, Transition Metal Carbides and Nitrides,
Acad. Press (1971).

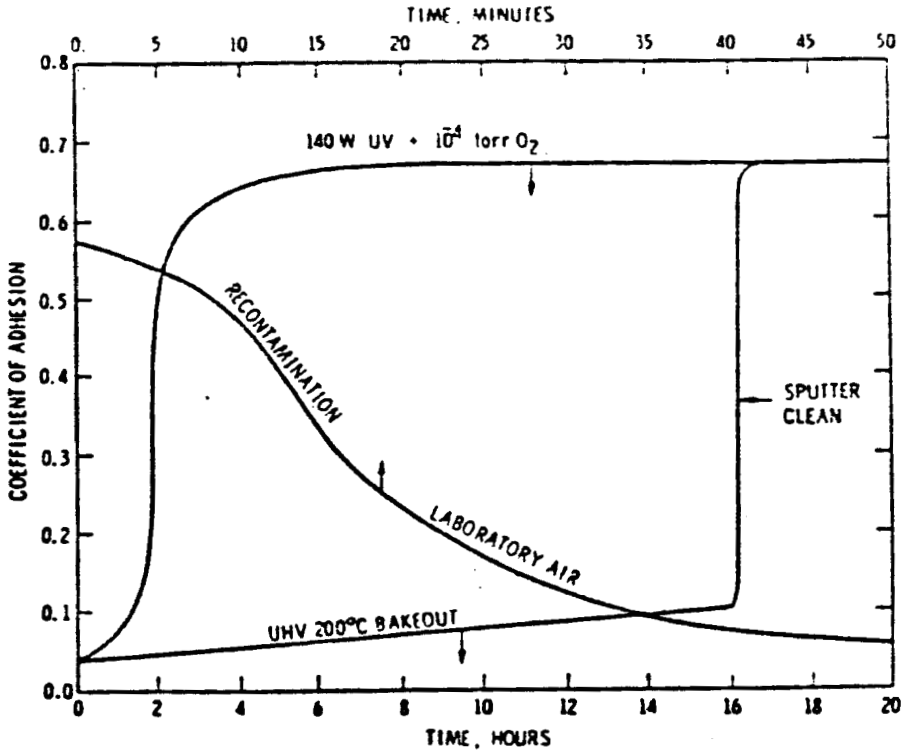

Figure 1. Cleaning of a gold surface by UHV 200°C bakeout, argon sputter cleaning, and UV irradiation at 10^{-4} Torr (lower scale). Recontamination rate in normal laboratory air is also shown (upper scale) (from reference 2).

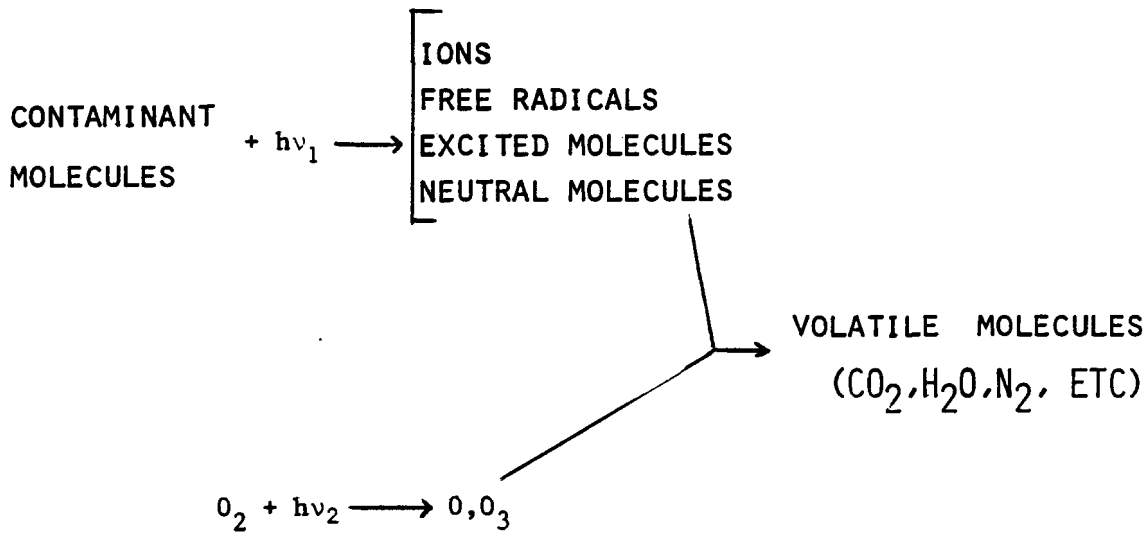

Figure 2 - Simplified schematic representation of UV/Ozone cleaning process.

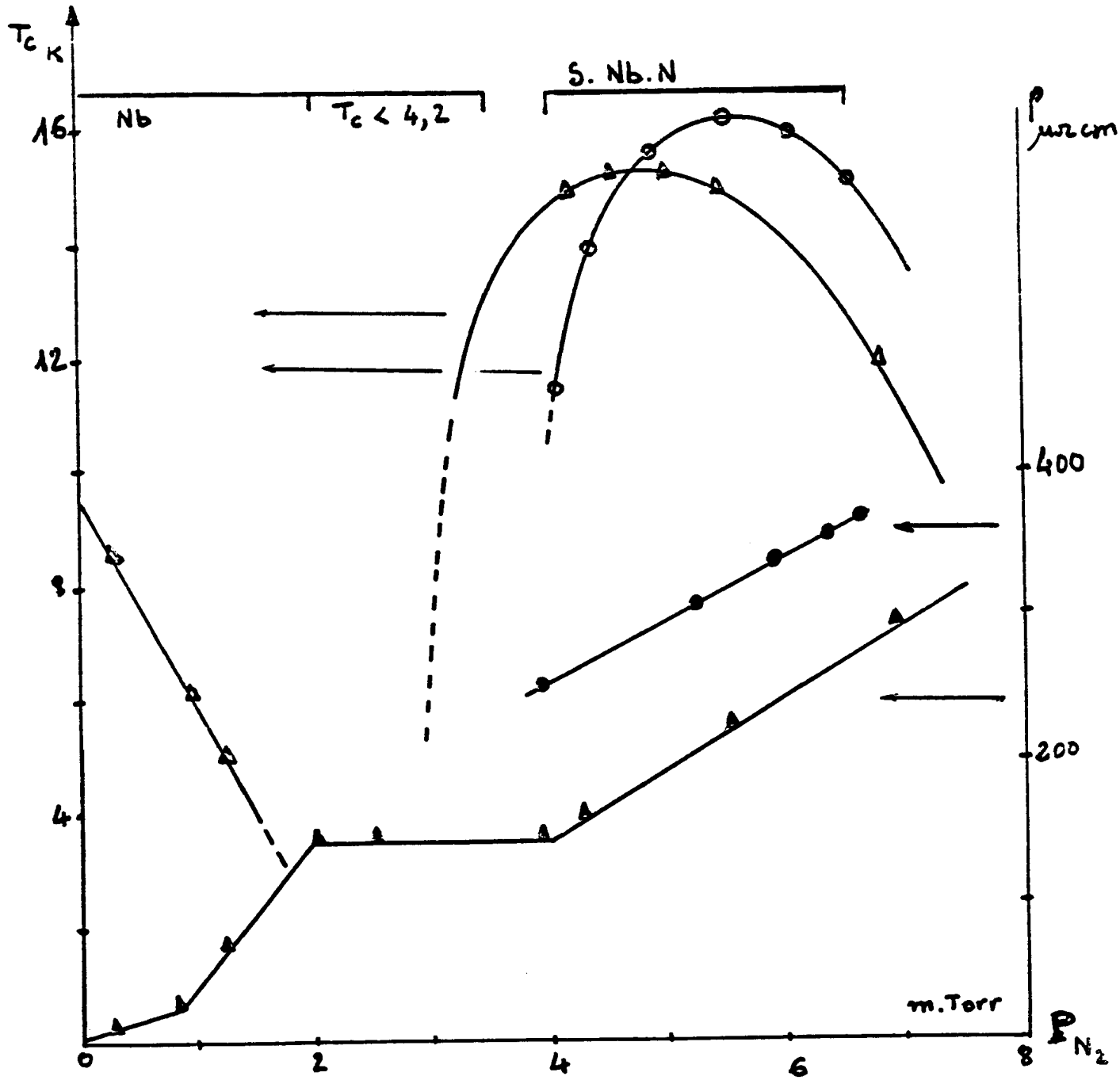

Figure 3 : Critical temperature and low temperature resistivity versus N_2 pressure during sputtering (Δ for P_{Argon} = 5 m torr ; 0 : P_{AR} = 15 m torr)

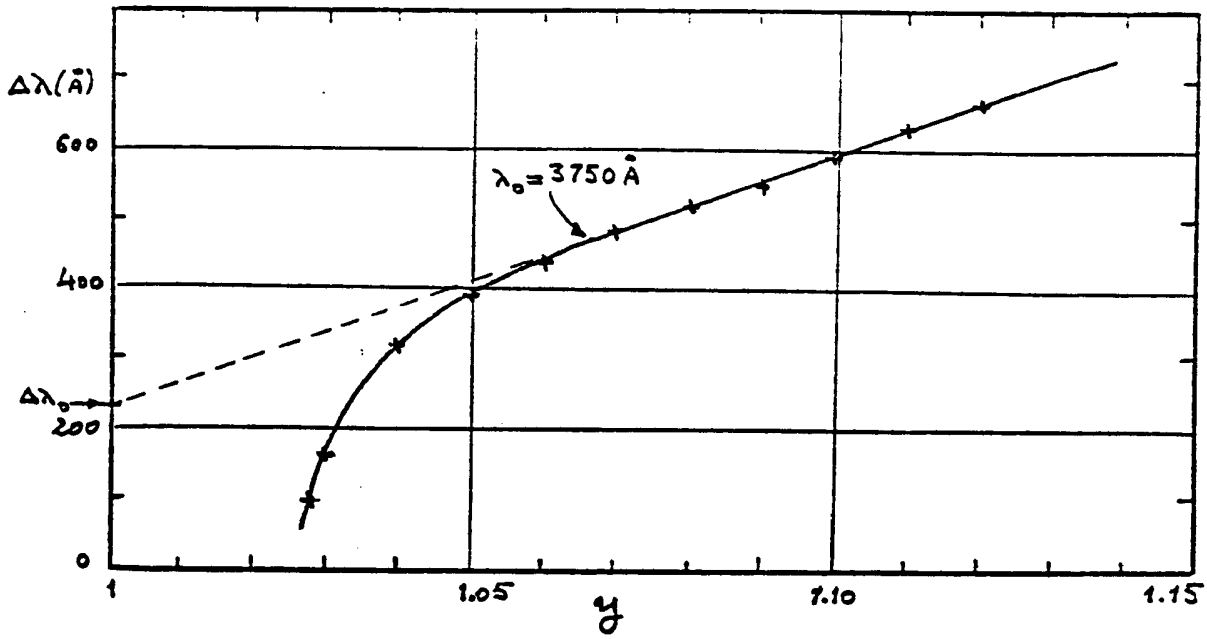

Figure 4 : Change of penetration depth versus $y = 1/\sqrt{1-(T/T_c)^4}$

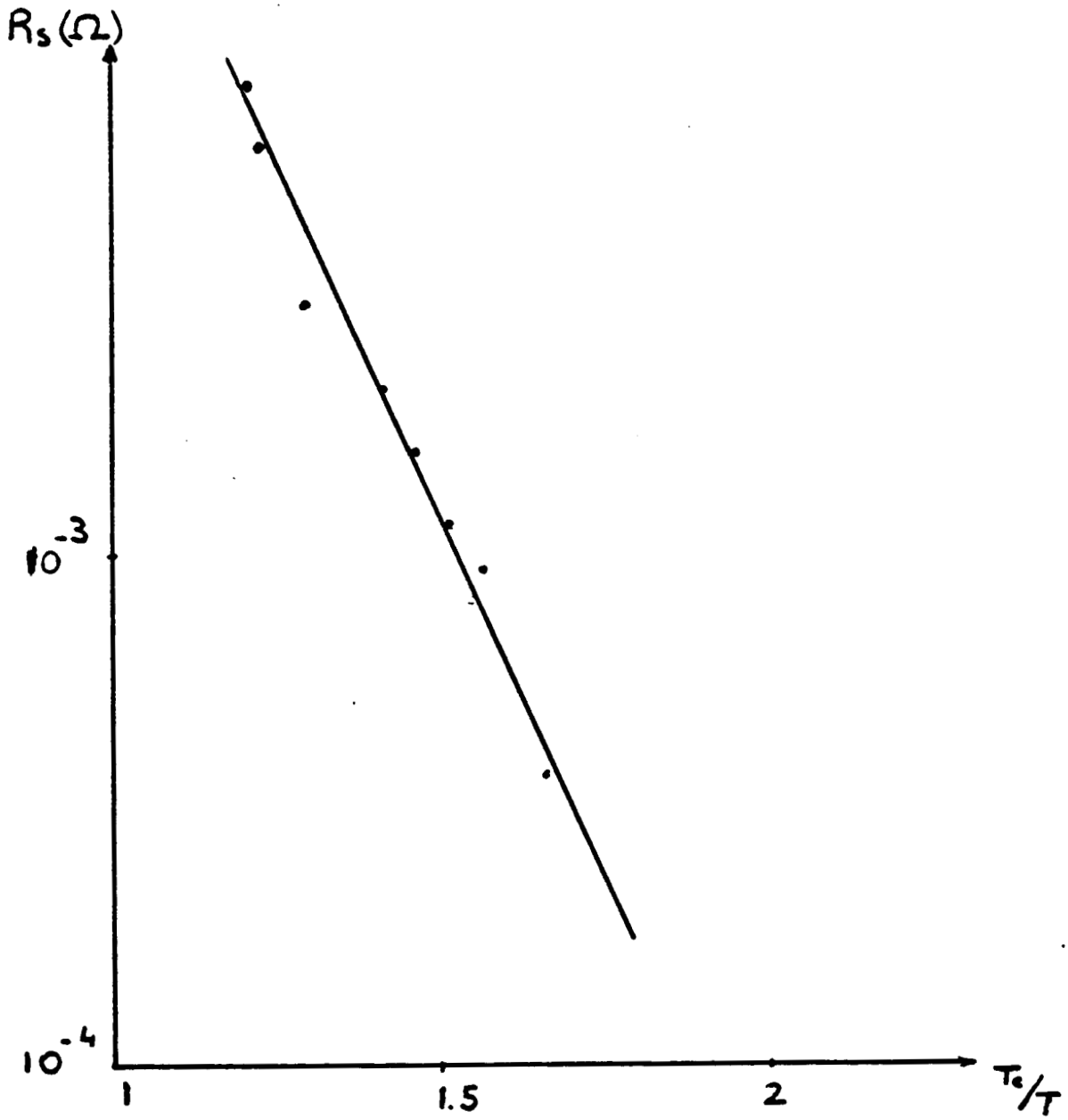

Figure 5 : NbN surface resistance versus the inverse reduced temperature.